A Novel Riemannian Metric for Geodesic Tractography in DTI

Andrea Fuster, Antonio Tristan-Vega, Tom Dela Haije, Carl-Fredrik Westin, and Luc Florack

Abstract One of the approaches in diffusion tensor imaging is to consider a Riemannian metric given by the inverse diffusion tensor. Such a metric is used for white matter tractography and connectivity analysis. We propose a modified metric tensor given by the adjugate rather than the inverse diffusion tensor. Tractography experiments on real brain diffusion data show improvement in the vicinity of isotropic diffusion regions compared to results for inverse (sharpened) diffusion tensors.

1 Introduction

In the Riemannian framework for diffusion tensor imaging (DTI) [3] white matter is represented as a Riemannian manifold and neural fibres are conjectured to coincide with certain geodesic curves[1] (shortest paths in a non-Euclidean sense). In this way the problem of tractography becomes one of finding geodesics. This is attractive from a practical point of view, as it obviates the need for ad hoc stopping and bending criteria necessary in traditional fibre-tracking algorithms.

[1]Classification of geodesics as fibres requires additional connectivity measures [1, 16].

A. Fuster (✉) · T. Dela Haije · L. Florack
Eindhoven University of Technology, Eindhoven, The Netherlands
e-mail: A.Fuster@tue.nl; T.C.J.Dela.Haije@tue.nl; L.M.J.Florack@tue.nl

A. Tristan-Vega
University of Valladolid, Valladolid, Spain
e-mail: atriveg@eii.uva.es

C.-F. Westin
Harvard Medical School, Boston, MA, USA
e-mail: westin@bwh.harvard.edu

T. Schultz et al. (eds.), *Computational Diffusion MRI and Brain Connectivity*, Mathematics and Visualization, DOI 10.1007/978-3-319-02475-2_9,

Finally, it has the conceptual advantage that Riemannian geometry is a well-understood and powerful theoretical machinery, facilitating mathematical modeling and algorithmics [1, 2, 6, 11, 13, 14, 16]. However, there are problematic aspects to the existing formulation of the Riemannian paradigm [11, 13]. The appealing idea is to transform anisotropic diffusion in Euclidean space to free Brownian diffusion in a curved Riemannian space. However, this is *not* achieved with the usual definition, in which the metric is identified with the inverse diffusion tensor. A related problem is that the standard metric does not favor tracts through anisotropic diffusion regions over tracts through isotropic ones, making masking a necessary preprocessing step in geodesic tractography.

In this paper we reconsider the relation between the DTI tensor and the Riemannian metric tensor. The question of how to choose an appropriate metric has been recently addressed [8, 9]. Below we stipulate a novel Riemannian metric that does yield Brownian motion in the corresponding curved space. We investigate the practical implications of the proposed metric on geodesic tractography by performing experiments on real brain diffusion data. We contrast our results with geodesic curves obtained from the inverse (sharpened) diffusion tensor. Experiments show that in our approach tracts avoid isotropic diffusion regions such as ventricles.

2 Theory

2.1 Preliminaries

We use the following notation and conventions. D^{ij}: diffusion tensor, D_{ij}: inverse of D^{ij}, $d = \det D^{ij}$, g_{ij}: metric tensor, g^{ij}: inverse of g_{ij}, $g = \det g_{ij}$, $\partial_i = \partial/\partial x^i$. A linear diffusion generator $\mathscr{L}$ is a differential operator of the form[2]

$$\mathscr{L} = a^{ij}(x)\partial_i\partial_j + b^i(x)\partial_i \tag{1}$$

where $a^{ij}(x)$ and $b^i(x)$ are smooth functions and a^{ij} is a symmetric positive definite tensor, with inverse a_{ij}. If we define a Riemannian metric on M as $g_{ij}(x) = a_{ij}(x)$, then we can rewrite $\mathscr{L}$ as

$$\mathscr{L} = \triangle_g + B \tag{2}$$

where $B = B(a^{ij}(x), b^i(x))$ is a smooth vector field and $\triangle_g$ is the Laplace-Beltrami operator w.r.t. the metric g_{ij}:

[2] We use Einstein's summation convention: $a_i b^i \stackrel{\text{def}}{=} \sum_i a_i b^i$.

$$\triangle_g = \frac{1}{\sqrt{g}}\,\partial_j\left(\sqrt{g}g^{ij}\partial_i\right) = g^{ij}\partial_i\partial_j + \frac{1}{\sqrt{g}}\,\partial_j\left(\sqrt{g}g^{ij}\right)\partial_i \tag{3}$$

The operator $\mathscr{L}$ is said to be an intrinsic Laplacian if $B = 0$. By definition, an intrinsic Laplacian generates Brownian motion on (M, g) [4]. However, with the usual identification $g^{ij} = D^{ij}$, the standard anisotropic diffusion generator yields

$$\mathscr{L}_1 = \partial_i(D^{ij}\partial_j) = D^{ij}\partial_i\partial_j + (\partial_j D^{ij})\partial_i = \triangle_g + \frac{1}{2d}\left(\partial_j d\right)D^{ij}\partial_i \tag{4}$$

where $B = (1/2d)\left(\partial_j d\right)D^{ij}\partial_i$, which generally does not vanish (unless d is constant). We conclude that this operator is *not* an intrinsic Laplacian and therefore the diffusion process associated with $\mathscr{L}_1$ is *not* a Brownian motion on (M, g). This discrepancy has not been signalled before in the literature.

2.2 Riemannian Framework Revisited

We propose to modify the Riemannian framework for DTI in such a way that the diffusion process associated with the diffusion generator is a Brownian motion on $(M, \tilde{g})$, for a certain Riemannian metric $\tilde{g}$. We consider metrics which are conformally equivalent to $g = D^{-1}$, i.e.

$$\tilde{g}_{ij} = f(x)D_{ij} \tag{5}$$

where $f(x)$ is a positive scalar function. The corresponding Laplace-Beltrami operator, Eq. (3), is

$$\triangle_{\tilde{g}} = \frac{1}{f}D^{ij}\partial_i\partial_j + \frac{1}{f}(\partial_j D^{ij})\partial_i + \frac{1}{2f}\left(\frac{1}{f}\partial_j f - \frac{1}{d}\partial_j d\right)D^{ij}\partial_i \tag{6}$$

Here we have used the relation $\tilde{g} = \det\,\tilde{g}_{ij} = f^3 d^{-1}$. This expression is similar to the anisotropic generator given by Eq. (4), except for an overall scaling factor of $1/f$ and the last term. The last term vanishes uniquely if $f \propto d$, and so without loss of generality we set $f = d$ so that $\tilde{g}_{ij} = d\ D_{ij}$, and

$$\mathscr{L}_2 \stackrel{\text{def}}{=} \triangle_{\tilde{g}} = d^{-1}D^{ij}\partial_i\partial_j + d^{-1}(\partial_j D^{ij})\partial_i \tag{7}$$

By construction the generator $\mathscr{L}_2$ is an intrinsic Laplacian. The diffusion process associated with $\mathscr{L}_2$ is thus a Brownian motion on $(M, \tilde{g})$. Therefore, we postulate the following Riemannian metric in the context of DTI:

$$\tilde{g}_{ij} = d\ D_{ij} \tag{8}$$

Recall that, for a regular square matrix A,

$$A^{-1} = \frac{1}{\det A} \operatorname{adj}(A) \tag{9}$$

with $\operatorname{adj}(A)$ the adjugate matrix. Thus the proposed metric is the adjugate of the diffusion tensor, rather than the inverse.

Note that the metric proposed in Hao et al. [8] is also of the form given by Eq. (5). In their case, the local factor is chosen so that geodesic curves more closely follow the diffusion tensor principal eigenvectors. Our metric, on the other hand, relates anisotropic diffusion in Euclidean space to isotropic diffusion in the corresponding Riemannian space. In sum, although both metrics are local rescalings of the inverse diffusion tensor they arise from rather distinct considerations.

3 Experiments

3.1 Method

We obtain geodesic curves from the inverse, inverse sharpened, and our newly proposed case, the adjugate diffusion tensor. In particular, we use a sharpened diffusion tensor [7]

$$(D_{\text{sharp}})^{ij} = d^{\frac{1-\alpha}{3}} (D^{ij})^{\alpha} \tag{10}$$

where $\alpha > 1$ is a constant. We take representative values $\alpha = 2, 4$ [10, 17]. In order to find the optimal geodesic[3] connecting a given target point to the seeding region we use the Fast-Sweeping algorithm in [12]. The algorithm assigns to each voxel the minimum cost of reaching it from a set of neighbours following predefined spatial orientations, provided that seeding points have zero cost. As local cost we use the infinitesimal curve length function:

$$L(\chi, \dot{\chi}) = (g_{ij}(\chi) \dot{\chi}^i \dot{\chi}^j)^{1/2} \tag{11}$$

where $\chi = \chi(t)$ is a curve parameterized by t, $\dot{\chi} = d\chi/dt$ is the tangent vector, and g_{ij} is the inverse, the inverse sharpened, or the adjugate of the diffusion tensor. The minimum cost and the spatial direction chosen are stored at each voxel. The set of preferred orientations comprise a vector field which may be "back-traced" (integrated) from the target to the seeding points to retrieve the desired geodesics. Recall that only a subset of geodesic curves corresponds to actual fibres; therefore we refer to geodesics either as candidate fibres, or simply as tracts.

[3] Here we consider the shortest geodesic between any given pair of points to be optimal.

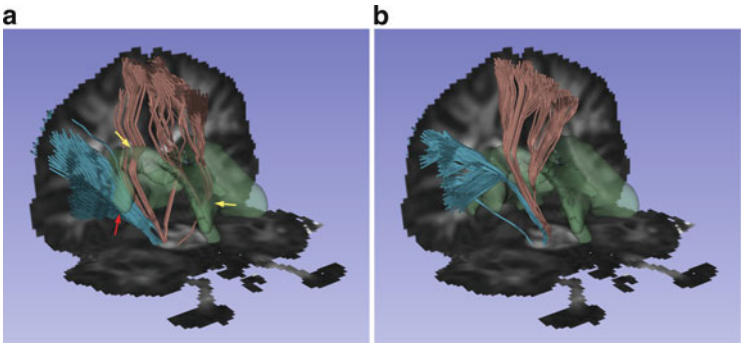

Fig. 1 Candidate fibres possibly corresponding to corticobulbar (*blue*) and corticospinal tracts (*brown*), in an anterior view. No candidate fibres shown in-between since we do not consider target points in that part of the cortex. A tumour is located next to the ventricles on the left-hand side. Results for metric given by (**a**) inverse diffusion tensor and (**b**) adjugate diffusion tensor. Candidate fibres going through the ventricles or the tumour are indicated by *yellow* and *red arrows*, respectively. Bundles obtained with our approach, in (**b**), avoid both the CSF in the ventricles and the tumour

3.2 Results

We consider a diffusion MRI data set with 64 gradient directions and a b-value of $3{,}000\,\mathrm{s/mm^2}$; the dimensions are $128 \times 128 \times 60$ and the voxel size is $1.75 \times 1.75 \times 2\,\mathrm{mm^3}$, corresponding to a patient with a tumor located next to the ventricles. We have segmented the cerebrospinal fluid (CSF) inside the ventricles, together with the tumour. We seed from the cerebral peduncles to a number of target points in the motor cortex, and visualize the obtained tracts using 3D Slicer [15].

In Figs. 1 and 2 we show candidate fibres reaching the trunk and foot motor area of the cortex (upward bundle) and the lip area (bundle bending to the left), which ought to correspond to the corticospinal and corticobulbar tracts. In Fig. 1 we show tractography results for metrics given by the inverse and adjugate diffusion tensor, and the outcome for inverse sharpened diffusion tensors is given in Fig. 2. Results obtained with our approach, Fig. 1b, seem to better resemble the anatomy of the stipulated white matter bundles. Additionally, the curvature of the candidate fibres is smoother and the bundles are more coherent. A particularly interesting result is the fact that our candidate fibres circumvent the ventricles, known to be void of fibres, while most of the ones obtained with other approaches go through them. Note that for sharpened tensors, Fig. 2, less bundles cross the CSF than in the original diffusion tensor case, Fig. 1a. Still, the problem is not completely overcome, as it is the case in our approach, Fig. 1b.

In Figs. 1 and 2 we also see that our tracts do not go through the tumour. This is consistent with our findings concerning the CSF since diffusion in tumours is usually also isotropic. Our results may reflect real fibres being pushed aside by a tumour, or white matter integrity inside the tumour having been destroyed.

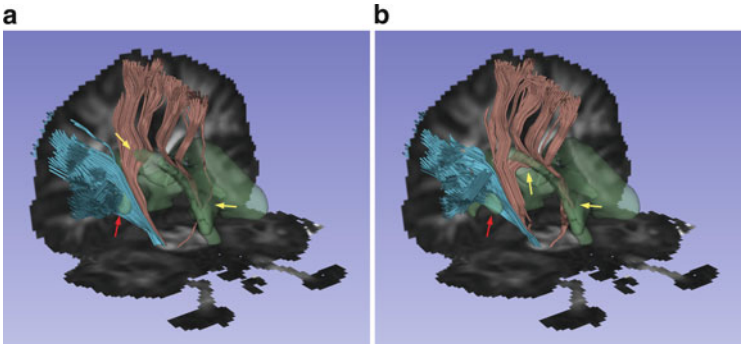

Fig. 2 As in Fig. 1, but now showing results for metric given by (**a**) inverse sharpened diffusion tensor $d^{1/3}D^{-2}$ and (**b**) inverse sharpened diffusion tensor dD^{-4} ($d = \det D$). Note that results from sharpened tensors improve compared to those without sharpening in Fig. 1a (i.e., less tracts cross isotropic diffusion regions), but the problem is not completely overcome as in our approach

In contrast to the ventricles case however, fibres might be found within a tumour and therefore we cannot draw any definitive conclusions about the validity of our results in this sense.

4 Conclusion and Discussion

We propose a new Riemannian metric in the context of DTI. We show results of geodesic tracking on real brain diffusion data, based on different ways to extract the Riemannian metric from the diffusion tensor. Tracts obtained with our approach avoid the encountered isotropic diffusion regions such as ventricles. Experiments show that this is not the case for some popular metrics proposed in the literature, including those involving heuristic diffusion tensor sharpening. It would be interesting to compare our method to the deconvolution sharpening in Descoteaux et al. [5]. Another known drawback of geodesic tractography based on the inverse diffusion tensor is the fact that geodesic curves tend to take shortcuts in the case of high-curvature tracts. In future work we will evaluate our metric in relation to this problem.

In summary, while masking has been necessary in (geodesic) tractography to avoid shortcuts through isotropic diffusion regions, our approach obviates such a preprocessing step as this is taken care of in an elegant way by the rigorously defined Riemannian metric. Finally, while in this work we only consider the effects on tractography, the choice of metric will also influence connectivity indices and Riemannian scalar measures in DTI [2].

Acknowledgements Tom Dela Haije gratefully acknowledges The Netherlands Organisation for Scientific Research (NWO) for financial support. Andrea Fuster would like to thank Lauren O'Donnell for feedback on brain white matter anatomy and Ana Achúcarro.

References

1. Astola, L., Florack, L., ter Haar Romeny, B.M.: Measures for pathway analysis in brain white matter using diffusion tensor images. In: Karssemeijer, N., Lelieveldt, B.P.F. (eds.) Proceedings of the IPMI 2007, Kerkrade. Lecture Notes in Computer Science, vol. 4584, pp. 642–649. Springer (2007)
2. Astola, L., Fuster, A., Florack, L.: A Riemannian scalar measure for diffusion tensor images. Pattern Recognit. **44**(9), 1885–1891 (2011)
3. Basser, P.J., Mattiello, J., Le Bihan, D.: Estimation of the effective self-diffusion tensor from the NMR spin echo. J. Magn. Reson. **103**, 247–254 (1994)
4. de Lara, M.C.: Geometric and symmetry properties of a nondegenerate diffusion process. Ann. Probab. **23**(4), 1557–1604 (1995). doi:10.1214/aop/1176987794. http://projecteuclid.org/euclid.aop/1176987794
5. Descoteaux, M., Deriche, R., Lenglet, C.: Diffusion tensor sharpening improves white matter tractography. In: SPIE Image Processing: Medical Imaging, San Diego, pp. 1084–1087 (2007)
6. Fletcher, P.T., Joshi, S.: Riemannian geometry for the statistical analysis of diffusion tensor data. Signal Process. **87**(2), 250–262 (2007)
7. Fletcher, P.T., Tao, R., Jeong, K.W., Whitaker, R.T.: A volumetric approach to quantifying region-to-region white matter connectivity in diffusion tensor MRI. In: Karssemeijer, N., Lelieveldt, B.P.F. (eds.) Proceedings of the IPMI 2007, Kerkrade. Lecture Notes in Computer Science, vol. 4584, pp. 346–358. Springer (2007)
8. Hao, X., Whitaker, R.T., Fletcher, P.T.: Adaptive Riemannian metrics for improved geodesic tracking of white matter. In: Székely, G., Hahn, H.K. (eds.) Proceedings of the IPMI 2011, Kloster Irsee. Lecture Notes in Computer Science, vol. 6801, pp. 13–24. Springer, Berlin (2011)
9. Jbabdi, S., Bellec, P., Toro, R., Daunizeau, J., Pélégrini-Issac, M., Benali, H.: Accurate anisotropic fast marching for diffusion-based geodesic tractography. Int. J. Biomed. Imaging **2008**, 1–12 (2008). doi:10.1155/2008/320195. http://www.hindawi.com/journals/ijbi/2008/320195/
10. Lazar, M., Weinstein, D.M., Tsuruda, J.S., Hasan, K.M., Arfanakis, K., Meyerand, M.E., Badie, B., Rowley, H.A., Haughton, V., Field, A., Alexander, A.L.: White matter tractography using diffusion tensor deflection. Hum. Brain Mapp. **18**(4), 306–321 (2003). doi:10.1002/hbm.10102. http://dx.doi.org/10.1002/hbm.10102
11. Lenglet, C., Deriche, R., Faugeras, O.: Inferring white matter geometry from diffusion tensor MRI: application to connectivity mapping. In: Pajdla, T., Matas, J. (eds.) Proceedings of the 8th European Conference on Computer Vision, Prague, May 2004. Lecture Notes in Computer Science, vol. 3021–3024, pp. 127–140. Springer, Berlin (2004)
12. Melonakos, J., Pichon, E., Angenent, S., Tannenbaum, A.: Finsler active contours. IEEE Trans. Pattern Anal. Mach. Intell. **30**(3), 412–423 (2008)
13. O'Donnell, L., Haker, S., Westin, C.F.: New approaches to estimation of white matter connectivity in diffusion tensor MRI: elliptic PDEs and geodesics in a tensor-warped space. In: Proceedings of Medical Imaging, Computing and Computer Assisted Intervention, Tokyo. Lecture Notes in Computer Science, vol. 2488, pp. 459–466. Springer (2002)
14. Pennec, X., Fillard, P., Ayache, N.: A Riemannian framework for tensor computing. Int. J. Comput. Vis. **66**(1), 41–66 (2006)
15. Pieper, S., Halle, M., Kikinis, R.: 3D Slicer. In: IEEE International Symposium on Biomedical Imaging ISBI 2004, Arlington, pp. 632–635 (2004)

16. Prados, E., Soatto, S., Lenglet, C., Pons, J.P., Wotawa, N., Deriche, R., Faugeras, O.: Control theory and fast marching techniques for brain connectivity mapping. In: Proceedings of the IEEE Computer Society Conference on Computer Vision and Pattern Recognition, New York, June 2006, vol. 1, pp. 1076–1083. IEEE Computer Society (2006)
17. Tournier, J.D., Calamante, F., Gadian, D.G., Connelly, A.: Diffusion-weighted magnetic resonance imaging fibre tracking using a front evolution algorithm. NeuroImage **20**(1), 276–288 (2003). doi:10.1016/S1053-8119(03)00236-2. http://www.sciencedirect.com/science/article/pii/S1053811903002362